International Journal of Thermal Sciences 49 (2010) 443–453

Contents lists available at ScienceDirect

International Journal of Thermal Sciences

journal homepage: www.elsevier.com/locate/ijts

# Numerical study of $NO_x$ formation during incineration of cellulosic and plastic materials: The combustion regime

Thomas Rogaume [a,*], Franck Richard [a], Timoléon Andzi Barhe [a], Jose L. Torero [b], Patrick Rousseaux [a]

[a] Laboratoire de Combustion et de Détonique, ENSMA, BP 40109, 86961 Futuroscope Cedex, France
[b] School of Engineering and Electronics, The University of Edinburgh, Edinburgh EH9 3JN, United Kingdom

ARTICLE INFO

*Article history:*
Received 24 October 2008
Received in revised form
10 July 2009
Accepted 22 July 2009
Available online 6 September 2009

*Keywords:*
$NO_x$ formation
Chemical pathways
Excess air

ABSTRACT

A numerical model has been developed (Chemkin) to study combustion processes in a fixed-bed reactor. The test section is divided into several successive Perfect Stirred Reactor (PSR). At the entry, the thermal degradation species of the solid are used as input and at the exit the exhaust gases are recovered. Comparison of previously experimental results and the current model output has been compared with good agreement. The model has been used to establish the reaction pathways at different locations in the reactor. This has allowed defining what is occurring at each specific location of the reactor. A sensitivity study has been conducted varying the different operating parameters. The reaction pathways and sensitivity study have shown that the production of NO is controlled mostly by local oxygen concentration, thus the location of the NO production region depends mostly on the primary air injection. Temperature can have a significant effect on the global NO output, but only if enough oxygen is available for the reactions to proceed. Reduction reactions appear almost insensitive to temperature.



## 1. Introduction

Incineration is one of the most commonly employed treatment processes for Municipal Solid Waste (MSW) in Europe, mainly because it allows a reduction of 70% of the mass and 90% of the volume of the waste. However, the biggest challenge for incineration remains on the transfer of pollution from the waste to the air, either through gaseous emissions or ashes. Among the major environmental concerns related to incineration are the emissions of nitrogen oxides ($NO_x$). $NO_x$ has been shown to contribute strongly to the formation of acid rain and photochemical smog [1].

During the incineration of municipal solid waste in grid furnace incinerators, NO is the major component of the $NO_x$ formed, representing 95% of those emissions [2]. Therefore, it is justifiable to concentrate only on the establishment of the main variables controlling NO. The main formation path, responsible for more than 95% of the nitrogen monoxide produced during incineration of MSW is through the fuel-NO mechanism. Incinerator temperatures are in the range of 1173–1323 K [3,4], and combustion is generally lean (typical residual oxygen levels range between 6 and 12%) therefore the quantity of NO formed by means of the thermal and prompt mechanisms can be neglected [5,6].

The formation of NO from the fuel has been well described in the past [5,7,8] leading to the development of general mechanism of formation for NO [7], nevertheless the specific paths to be followed are affected both by the nature of the fuel and the conditions of combustion.

The pyrolysis process defines the global concentration of reactants, but the production of the different species is also influenced by local combustion conditions. In particular, the fuel-NO mechanism is principally controlled by the local oxygen concentration [5–7]. Optimisation of the combustion process therefore requires management of both the fuel gasification conditions and the detail knowledge of the principal reactive zones of a furnace. The detailed information required for optimal burning conditions continues to remain generally unavailable for MSW incinerators.

Characterization of the pyrolysis process and the subsequent fuel input into the gas phase for the model MSW of this study was conducted together with a general description of the reactive zones [8]. The authors established three distinctive combustion regimes defined by the global equivalence ratio at the onset of the combustion process. In a later study, a numerical model was developed and validated to attempt prediction of different pollutant species [9,10]. The present study extends the past work [9,10], to study the different chemical reaction pathways leading to the formation of NO as a function of the different combustion regimes present in a furnace. The fuel remains the model MSW

* Corresponding author. Tel.: +33 549 49 82 90; fax: +33 549 08 23 36.
*E-mail address:* trogaume@univ-poitiers.fr (T. Rogaume).

1290-0729/$ – see front matter © 2009 Elsevier Masson SAS. All rights reserved.
doi:10.1016/j.ijthermalsci.2009.07.028

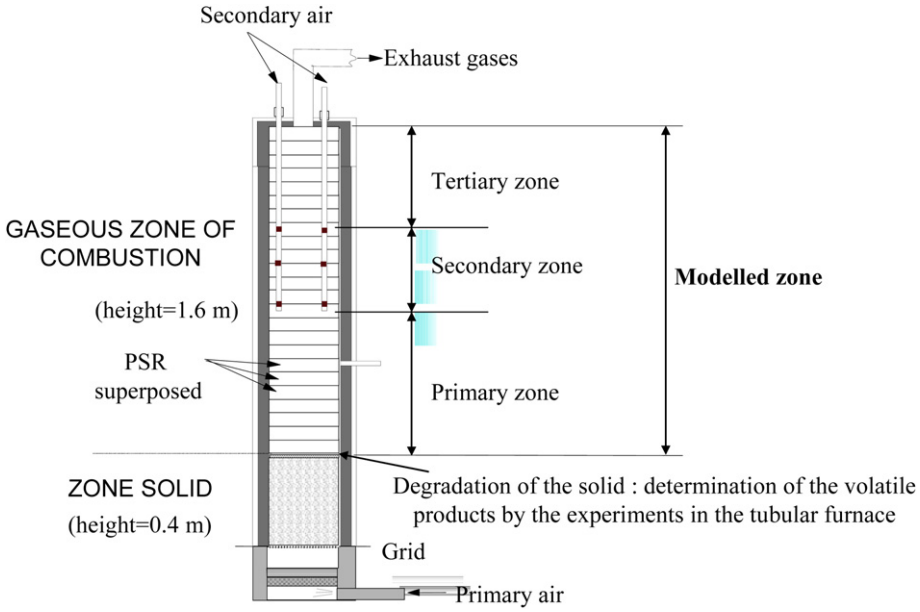


**Fig. 1.** Schematic of the reactor indicating the basic structure used for the model.

described in Ref. [8] and the air supply is the main operational parameter studied.

## 2. The combustion model

The architecture of the model has been presented in detail in Refs. [9,10] and only a brief summary will be presented here. The model allows simulating the combustion process in a counter flow fixed-bed reactor (Fig. 1). Details on the reactor characteristics and experimental procedures can be found [8].

The analytical study of a solid waste incinerator is strongly limited by the uncertainty in fuel composition and by the complexity of the different processes involved. A conventional way of conducting a parametric study of the different processes affecting waste incineration relies on the use of a standardised fuel and a geometry that enables good control and repeatability. For this study the fuel is generated in the laboratory with a mass composition that is representative of typical European municipal waste, composed of 41% of wood, 37% of cardboard, 19% of PET and 3% of polyamide.

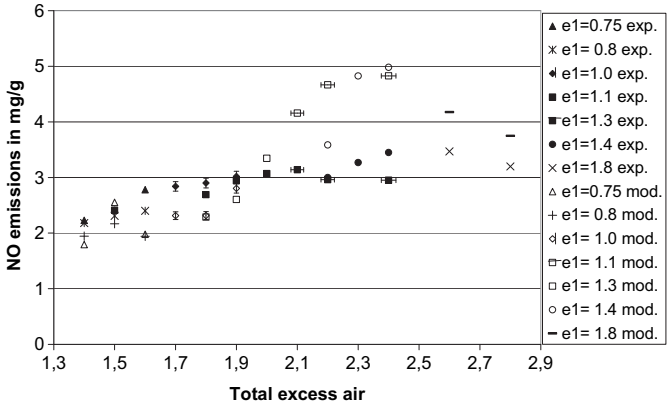


**Fig. 2.** Comparison of the measured and predicted NO profiles as a function of the total excess air.

It is usually assumed that combustion of MSW can be divided into three steps [8,11,12]: degradation of the waste, combustion of volatile gases and char burnout. For the present fuel the degradation step can be considered as pure pyrolysis with little or no heterogeneous oxidation present [8]. The combustion of the volatile gases takes place in three different reactive zones (Fig. 1): the primary zone where the products of pyrolysis burn with the primary air (introduced through the fuel), the secondary zone, where the products issue from the primary zone burn with the secondary air (introduced through ports axially distributed), and a tertiary zone or cool down region where the combustion ends. For modelling purposes fuel intake will be defined by pyrolysis and char burnout will be neglected and only the gas phase combustion will be described by the model [8,9].

Detailed modelling of both chemistry and transport is of extreme complexity for these reactors and generally requires extremely long computations. The benefit of this type of models is nevertheless not clear since the assumptions, related to both transport and kinetics, tend to be very strong. It is therefore common practice to simplify those processes that are deemed to have a lesser effect on the variables to be studied, in this case $NO_x$ production.

In the case of nitrogen oxide formation reactions, a detailed chemistry is needed [13]. Furthermore Vitali et al. [14] working on the optimisation of re-burning via modelling, demonstrated that a detailed chemical mechanism with a simplified representation of mixing can be used not only to explore the chemistry but also to identify ranges of process parameters that give optimum performance. This approach requires embedding all the necessary detail in the chemistry of formation/reduction of the $NO_x$. Following these conclusions, a detailed kinetic model is applied to a network of reactors where the flow field is not resolved. The literature cites several examples where this approach has been followed to predict the formation of $NO_x$ [12,15]. Each individual reactor corresponds to a separate disk and the input of one is the output of the one upstream, see Fig. 1. Transport within the reactor is simplified to a zero-dimensional flow and turbulence will be assumed to be homogeneous within each reactor. Each reactor can be then considered as an adiabatic Perfectly Stirred Reactor (PSR). The temperature in each PSR is fixed and computed from the

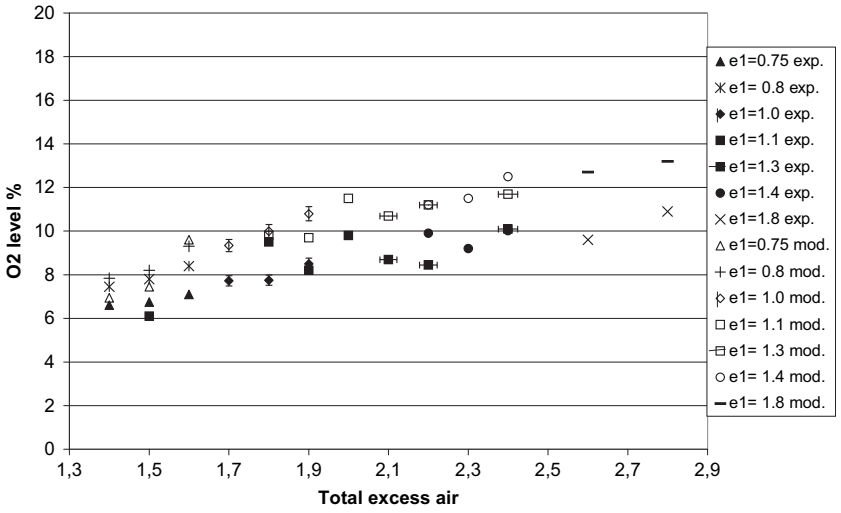


**Fig. 3.** Comparison of the measured and predicted residual oxygen concentration at the exit of the reactor and as a function of the total excess air.

experiments. The chemistry occurring within the reactor is established using Chemkin II [16].

It was established experimentally that the reactor temperature ranges between 1100 and 1300 K and the pressure can be considered to remain atmospheric [8]. The local equivalence ratio, in each different zone of combustion, is generally expected to range between 0.5 and 1.1. Although the experimental conditions show that the local global equivalence ratio ranges between 0.4 and 1.7, the local values affecting combustion are most likely situated between 0.5 and 1.1 [8]. Furthermore, it was shown that most of the gases introduced by pyrolysis are carbon oxides and light hydrocarbons ($CH_4$, $C_2H_2$, $C_2H_4$, $C_2H_6$) and hydrogen. Therefore, several kinetic models can be potentially used [7,17–19]. Nevertheless, the presence of aromatic compounds and small concentration of $C_3H_6$, $C_3H_8$ and $C_6H_6$ make necessary for the kinetic model to take into account these species. This limits the choice to the detailed kinetic model developed by Dagaut et al. [19]. This detailed reaction mechanism consists of 112 species involved into 892 reversible reactions. The dissociation reaction associated to $CH_3CONH_2$, which is a product of the pyrolysis of polyamide [20] has been added. Dagaut et al. [19] establish that the temperature of application of the model ranges between 1000 and 1450 K which is within the bounds of the experimental conditions, nevertheless the equivalence ratio for which the model has been validates is limited to 0.7–2.5 which overlaps but does not include the entire range of experimental values. This issue will be discussed in next sections.

A computer program was developed to make use of Chemkin II [16], together with the model for a PSR created by Glarborg et al. [21]. All results were obtained with at least 1000 PSR. This number was deemed as being sufficient to obtain independence of the results from this parameter [9]. For the reactors corresponding to the secondary air injection ports a special subroutine was written to distribute the air so that the residence time is consistent with the experimental conditions.

For initialisation, the program requires the knowledge of the volatile products generated by the thermal degradation of the solids. This composition forms the initial condition to start the simulation in the first PSR. The results given by this first disc (first PSR) are placed in a file and are the initial conditions for the second disc and so forth. The composition of the volatiles has been experimentally determined using a tubular furnace [9,10]. To define the concentrations of the components that could not be measured,

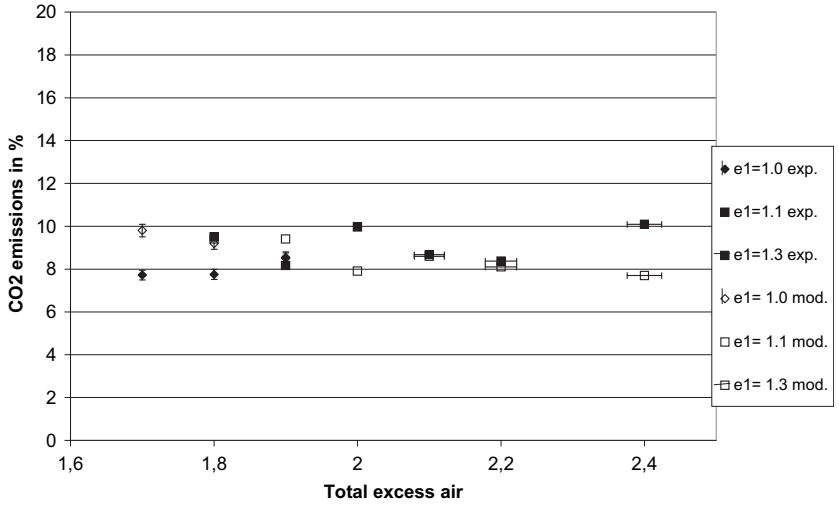


**Fig. 4.** Comparison of the measured and predicted $CO_2$ concentrations at the exit of the reactor and as a function of the total excess air.

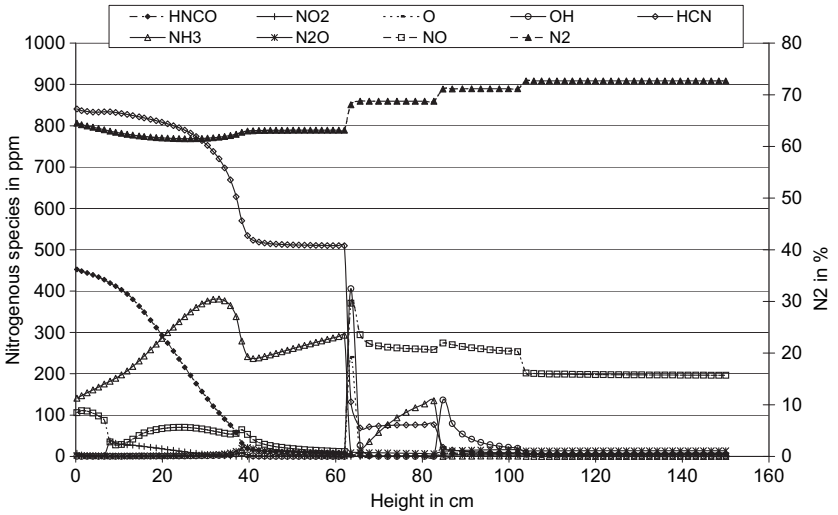


**Fig. 5.** Example of evolution of the nitrogenous species across the reactor for a primary excess air $e_1 < 1$.

values from the literature were incorporated. The complete reconstruction of the 1.4 kg of fuel present in the reactor is given in mol%. Therefore, the composition of the volatiles was defined as: 35.66% of CO, 5% of $CO_2$, 12.8% $CH_4$, 9% $C_6H_6$, 0.18% $CH_3CONH_2$, 0.4% HCN, 0.1% $NH_3$, 0.03% NO, 13.7% $H_2$, 0.23% HNCO, 22.9% OH (coming from the very fast reaction of dissociation of the water).

## 3. Experimental results and model validation

The numerical model was benchmarked against a series of experimental results obtained by Rogaume et al. [9,10]. Fig. 2 shows NO emissions as a function of the total excess air, $e_T$. The total excess air is obtained from the imposed flow rate and the rate of fuel consumption and is equal to (1/equivalence ratio). The rate of fuel consumption is a function of the primary air, thus needs to be defined from the experimental results.

The measured NO concentrations show good agreement with the model for $e_T \leq 2$ (Fig. 2). For $e_T > 2$ the model tends to over predict the NO concentration. As indicated in a previous section, the numerical code uses the kinetic model developed by Dagaut et al. [19] which has been validated for an equivalence ratio between 0.7 and 2.5, therefore it is not surprising that when the overall equivalence ratio goes below 0.5 ($e_T = 2$) errors can arise. These errors seem to be magnified when the local equivalence ratio in the secondary zone of combustion decreases keeping this region well below the minimum equivalence ratio for which the kinetic model has been validated. Although the results show over prediction of NO under certain flow conditions, model and experiments seem to follow similar trends and produce quantitatively similar results.

The results for the residual oxygen concentration are presented in Fig. 3. As expected, the amount of unused oxygen increases with the excess air in an almost linear fashion. The model predicts very well the trends but nevertheless consistently over predicts the oxygen concentration by approximately 15%. The over prediction could be attributed to further oxidation of the combustion products between the reactor and the analyzer. Temperatures at the exit of the reactor, which corresponds to the modelling domain, are still high and further oxidation could be expected.

The concentrations of $CO_2$ are presented for $1.7 \leq e_T \leq 2.4$ in Fig. 4. In this case, the range of excess air presented was limited to the conditions most commonly employed during the incineration of municipal solid waste. The results show good agreement between the measured $CO_2$ concentrations and the model. Furthermore, $CO_2$ concentrations remain almost constant indicating that, within the range of flow rates studied, carbon oxidation is not limited by oxygen supply but by the kinetics of the reaction.

## 4. Numerical results and discussion

Global measurements provide an indication of the effectiveness of the present model. Nevertheless, it is important to resolve the

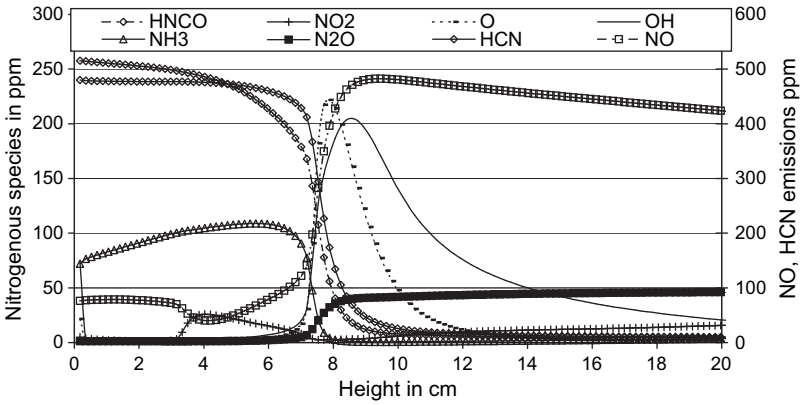


**Fig. 6.** Example of evolution of the nitrogenous species across the reactor for a primary excess air $e_1 \geq 1$ between the top of the bed to 20 cm up.

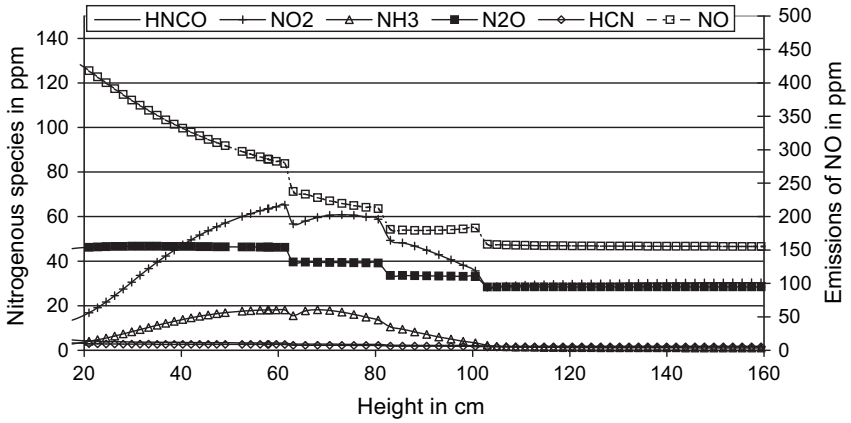


**Fig. 7.** Example of evolution of the nitrogenous species across the reactor for a primary excess air $e_1 \geq 1$ between 20 cm to the top of the bed to the exhaust gas.

local effects of primary and secondary injection. This is necessary because fuel NO production is strongly dependent on the local oxygen concentration. In this section the major rates of the different formation and consumption reactions for each species are presented to establish a map of all the intermediate species along the reactor. Three scenarios have been studied, $e_1 < 1$, $e_1 = 1$ and $e_1 > 1$, but $e_1 = 1$ and $e_1 > 1$ show very similar trends, therefore $e_1 = 1$ and $e_1 > 1$ will be grouped as a single case.

Figs. 5–7 present the evolution of the nitrogenous species as a function of the location in the reactor, with "0" being the fuel surface and "160" the exhaust of the reactor. The injection of the secondary air is staged in three levels located respectively at 63, 83 and 103 cm. The species shown are only those that are expected to play a significant role in the production of NO. Omitted from the plot are NCO, NH, HNO and $NH_2$ that are also recognised as important intermediary species to the production of NO. These radicals are not presented because their destruction rates are similar to their production rates, thus their concentrations cannot be tracked track.

Fig. 5 shows that for the case of $e_1 < 1$, the oxidation of nitrogenous species does not occur in the primary zone of combustion but takes place in the secondary one. The oxygen supplied to the reaction from the primary air injection is not sufficient for a complete oxidation of the pyrolysis products generated from the degradation of the fuel. At the first port of secondary air injection (63 cm) there is still significant concentrations of $NH_3$ and HCN. The oxidation is then mostly completed at the first port of secondary air injection with only $NH_3$ present downstream of this port. $NH_3$ will be fully consumed at the second port of secondary air injection (83 cm). The oxidation of $NH_3$ and HCN leads to the increase in NO and $N_2$ concentrations. Downstream the NO form will be slowly reduced to form $N_2$. After the third injection port the different species concentrations do not evolve anymore identifying the end of the combustion.

Figs. 6 and 7 show the evolution of the nitrogenous species for $e_1 \geq 1$ obtained under exactly the same conditions. Fig. 6 shows in detail the region close to the pyrolysis front, while Fig. 7 shows the region downstream of the primary zone of combustion.

Fig. 6 shows a first reacting zone that is characterized by the consumption of the primary products of pyrolysis via oxidation (HCN, HNCO and $NH_3$). This region corresponds to the first 12 cm above the pyrolysis zone. It can be seen that initially HCN and HNCO are consumed slowly ($\leq$6 cm). In this region, the concentration of $NH_3$ increases due to the decomposition of $CH_3CONH_2$. Approximately 6 cm downstream of the pyrolysis front there is an increase in concentration of O and OH radicals that will accompany the consumption of HCN, HNCO and $NH_3$ leading to the production of NO, $N_2O$ and $N_2$ [8]. In this zone it will be expected to see significant presence of NCO, NH, HNO and $NH_2$ that are important intermediates but being radicals, their destruction rates are similar to their

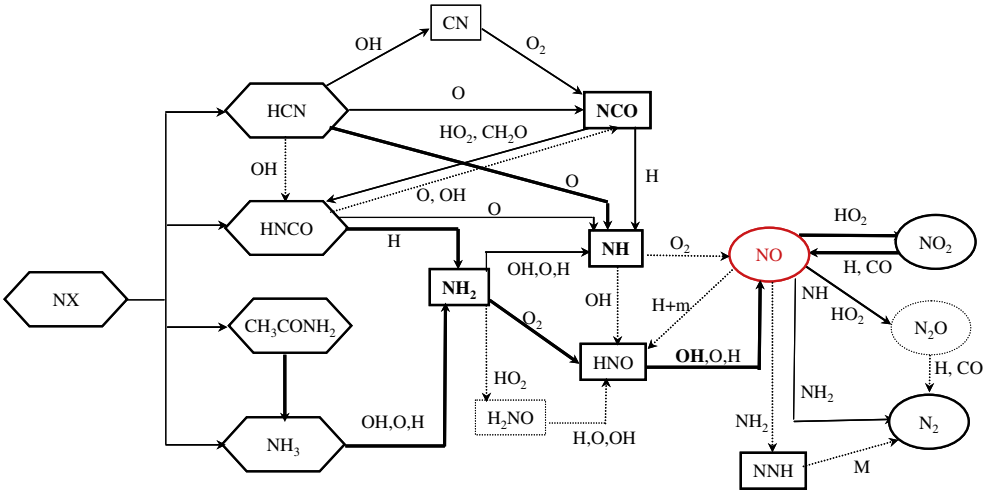


**Fig. 8.** Reacting schema of formation of NO and $N_2$ for $e_1 < 1$.

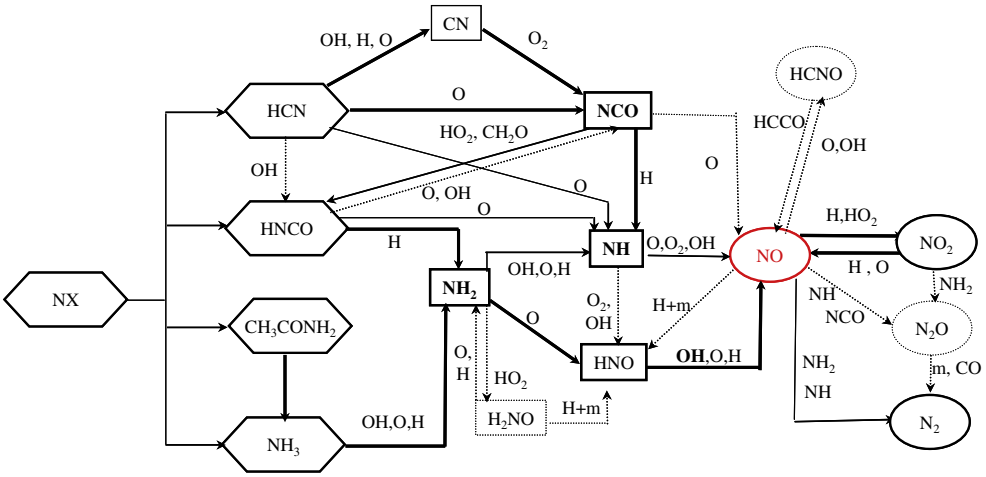


**Fig. 9.** Reacting schema of formation of NO and $N_2$ for $e_1 = 1$.

production rates, thus, cannot be tracked. It is important to notice that NO concentrations are higher than those of $N_2O$. This reinforces the theory that NO is first formed and then reacts to form $N_2O$ and $N_2$.

Between 12 and 60 cm, the concentration of the different intermediates is low, and their role is negligible. Indeed, once HCN and HNCO have been fully consumed a double path for the slow destruction of NO follows. On the one hand oxidation leads to the production of $N_2$ and $N_2O$ and reduction regenerates $NH_3$. The reduction of the emissions of NO takes place until the injection of the secondary air. A more detailed observation of the compounds present at this stage shows that reduction is achieved in the presence of the radicals $NH_2$, NH and NCO (see Figs. 8–13).

In the secondary zone of combustion, the production of $NO_2$ and $NH_3$ decreases together with a deceleration in the consumption of NO. Eventually, the concentrations of $NO_2$ and $NH_3$ start to decrease while the NO concentration attains a steady value. The injection of the secondary air leads to a reduction of the emissions of NO to form principally $N_2$. After the third injection port, the different species concentrations do not evolve anymore identifying the end of the combustion.

The above results have been used to identify possible reaction pathways for the formation and destruction of NO. The PSR gives as outputs the rates of all chemical reactions within the combustion mechanism. Therefore it is possible to determine the evolution of species from the calculation of the global rates of formation and consumption. The construction of the chemical pathways has been done using those global rates at each step of the reaction.

Following NO it was possible to determine the principal intermediates and reactions conducting to its formation or destruction and to back track these steps until reaching the original products of pyrolysis and inert species. The global reacting schemas for the different conditions are presented in Fig. 8 (for $e_1 < 1$), Fig. 9 (for $e_1 = 1$) and Fig. 10 (for $e_1 > 1$). The main reaction paths presented in these figures are summarized below.

As observed in Figs. 8–10, pyrolysis of the waste leads to the formation of HCN, $NH_3$, HNCO and $CH_3CONH_2$ (and directly a small part of NO). Those components react to form the principal intermediates that are NCO, NH and HNO. The reaction takes place mainly with the radicals O, OH, H coming from the dissociation of oxygen and water. Therefore, HNCO leads directly to the formation of NCO, HCN is oxidised to form NCO directly or through the formation of the radical CN and $NH_3$ reacts to form $NH_2$ resulting in the formation of NH and HNO. An increase of the oxygen concentration favours those reactions. The value of $e_1$ appears as the controlling parameter at this stage. For $e_1 < 1$, the single species

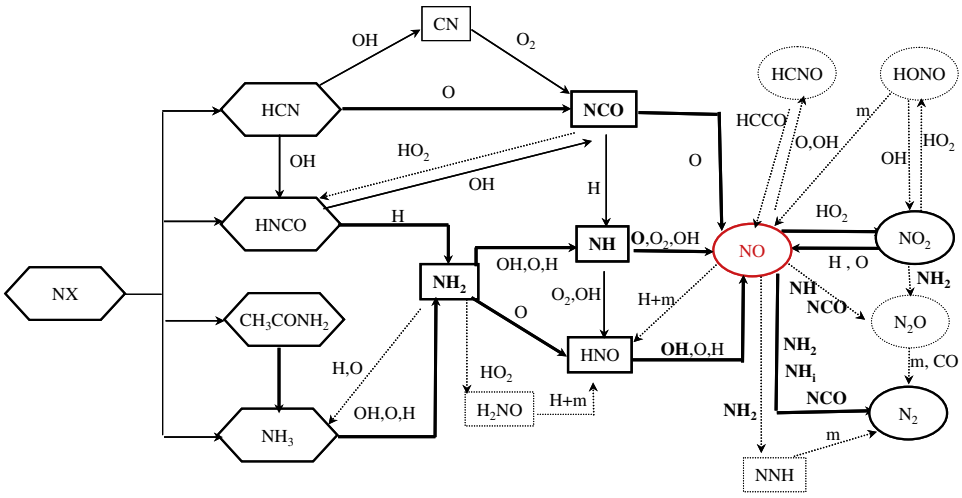


**Fig. 10.** Reacting schema of formation of NO and $N_2$ for $e_1 > 1$.

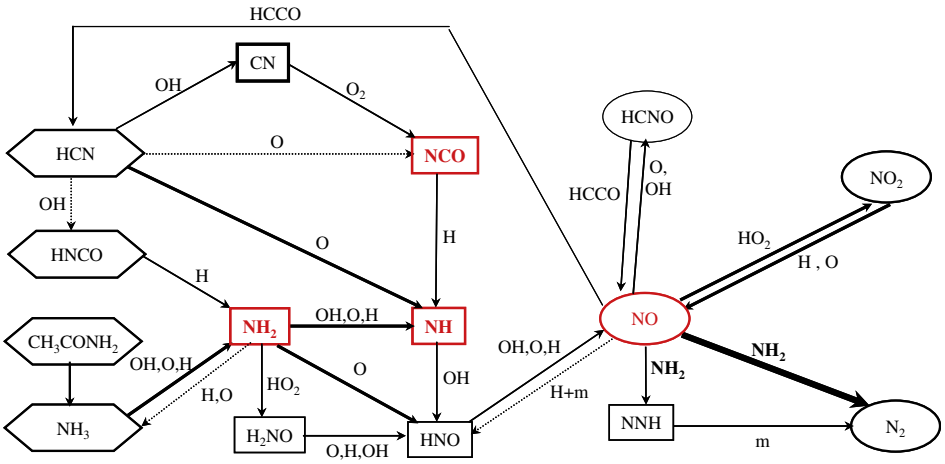


**Fig. 11.** Reacting schema of consumption of the NO for $e_1 < 1$.

conducting to NO is HNO, for $e_1 = 1$, HNO and NH are oxidised to form NO and for $e_1 > 1$, the HNO, NH and NCO already formed conduct directly to NO. Throughout these steps the dominant specie is the radical O, this highlights the importance of the local oxygen concentration on the followed reaction path. This result is consistent with the description of the yield of formation of NO through the fuel-NO mechanism described elsewhere [5].

During this phase of the production of NO, part of NO formed is converted to $N_2$. Nevertheless, the rate of consumption of NO is less important than its rate of production. We remark that $N_2$ is not formed directly from the products of degradation, but is formed from NO.

The discussion above strongly suggests that these processes are controlled by the availability of oxygen, thus, a spatial analysis of the reactor shows that for $e_1 < 1$ the production of NO is pushed towards the secondary zone of combustion, while for all other conditions it starts as soon as the pyrolysis gases leave the fuel.

As done before for NO formation, NO consumption can also be tracked and the resulting reaction pathways are presented in Figs. 11–13 for all three conditions of primary air injection. The consumption of NO is strongly dependent on the primary excess air. For $e_1 < 1$, NO is reduced mainly by reacting with $NH_2$, for $e_1 = 1$, NO conducts to $N_2$ by reacting with $NH_2$ and NH and for $e_1 > 1$, $NH_2$, NH and NCO react with NO to form $N_2$. Consumption occurs directly or through multiple steps leading to the formation of NNH and $N_2O$. NO can also react with HCCO and $CH_3$ produced from hydrocarbons oxidation to.

From the different schemes of NO destruction it is important to identify how the reducing species are generated. The main reducing species are $NH_2$ and NH, these are products of the oxidation of ammonia. Ammonia is a product of the fuel degradation and is generated by the dissociation of $CH_3CONH_2$. It is important to note that an alternative path for those species is to form HNO which in turn can be oxidised to form NO. Nevertheless, typical rates for these reactions are low thus formation of $NH_2$ and NH is favoured. The final reducing specie is NCO. NCO is generated by the oxidation of HNCO and HCN. This oxidation can be direct or through the intermediate specie CN. Local oxygen concentrations are again dominant in the reduction process. Higher is the value of the excess air and more directly those reactions take place.

Finally, it can be noted that NO is in equilibrium with $NO_2$. The equilibrium condition is directly dependant on the oxygen concentration. An increase of the oxygen concentration favours the formation of NO.

The destruction of NO occurs in two different locations. First, $N_2$ and $NO_2$ are formed from NO before the secondary air injection (between 12 and 63 cm). This reduction regenerates $NH_3$ and occurs in the presence of the radicals $NH_2$, NH and NCO for $e_1 > 1$ and only $NH_2$, NH for $e_1 = 1$. During this phase we notice the preponderance of a reducing atmosphere as well as the radical OH.

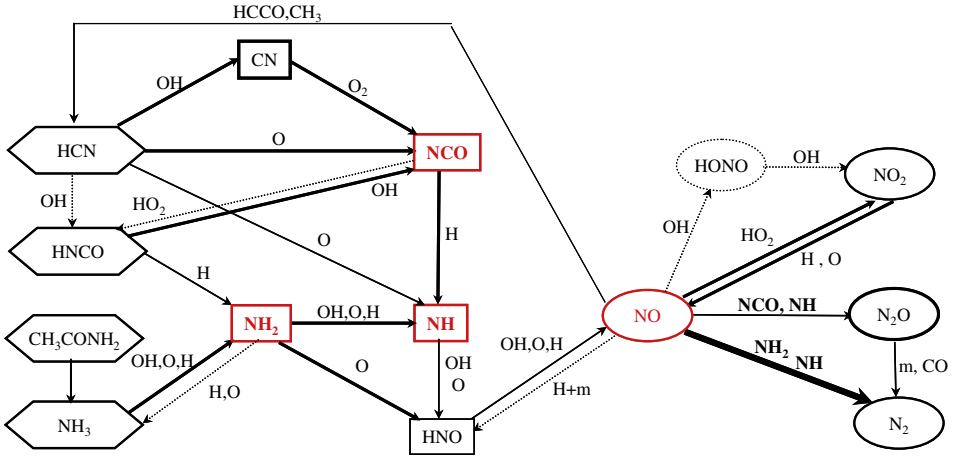


**Fig. 12.** Reacting schema of consumption of the NO for $e_1 = 1$.

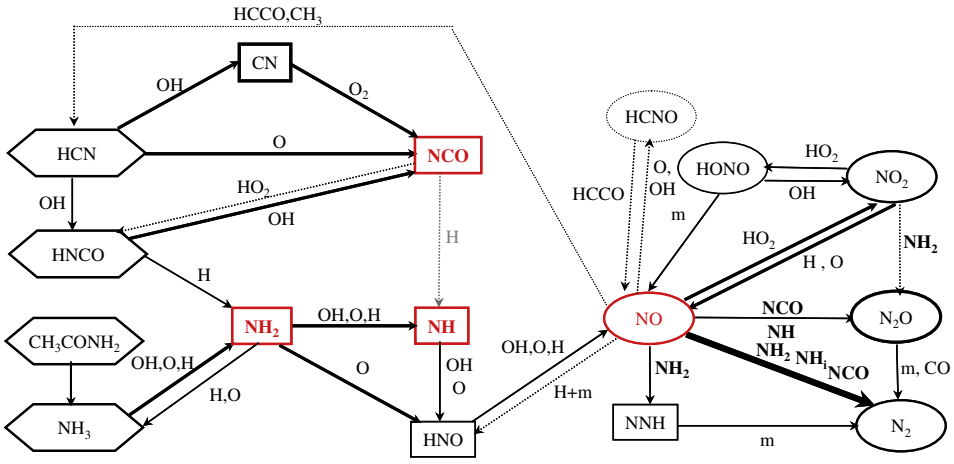


**Fig. 13.** Reacting schema of consumption of the NO for $e_1 > 1$.

In the secondary combustion zone (63–103 cm) the presence of oxygen favors the reduction of NO emissions but also the generation of NO through oxidation of the last incomplete products of combustion. The two different reactions lead to a net increase in the production of $N_2$.

The sensitivity to the different operational parameters on the NO emissions has been studied using the previously described model. For these experiments, fuel production is a function of the primary airflow therefore the primary and secondary excess air are dependent variables. Furthermore, the input parameters for the model include the local temperature, which is obtained from experimental values therefore cannot be modified. Here, twelve cases corresponding to experimental conditions have been modeled. The baseline conditions are summarized in Table 1 and they cover all regimes of primary air. For each condition one parameter will be varied systematically, leaving all other fixed to the experimental values. This allows to evaluate the influence of one input parameter for each regime, $e_1 < 1$, $e_1 = 1$ and $e_1 > 1$, without departing greatly from the experimental conditions.

The model was first used to obtain the evolution of the NO concentration at the outlet of the reactor as a function of the primary and secondary air flow rates. The fuel consumption rate and the temperatures for both reaction zones ($T_1$, $T_2$) are fixed to the experimental data and only the value of the primary airflow has been varied. Fig. 14 represents the evolution of the NO concentration at the outlet of the reactor as a function of the primary excess air. The full symbols corresponds to baseline experimental conditions where $e_1 < 1$, the empty symbols for $e_1 = 1$, and the lines for conditions typical of $e_1 > 1$. The horizontal axis corresponds to the evolution of $e_1$ when the primary airflow was systematically changed from the baseline condition.

Whatever the baseline condition, the evolution of NO emissions is qualitatively similar when $e_1$ is varied systematically. There are two well-defined combustion regimes that depend only on the value of the primary excess air. For $e_1 < 1$ the NO emissions are a decreasing function of the excess air. In those conditions, the local oxygen concentration in the primary zone of combustion is low. It does not permit a complete oxidation of the intermediate species, as NHi and HCN, therefore oxidation progresses to the secondary zone of combustion, as previously shown in Fig. 5. An increase of the primary excess air permits a better oxidation of the nitrogenous species in the primary zone producing NO. NO is then reduced in the secondary zone of combustion by reaction with reducing species (NH, $NH_2$, NCO). The overall production of NO is dominated by what happens in the secondary zone, therefore, the larger $e_1$ the more effective NO oxidation in the secondary zone. The result is NO production becoming a decreasing function of $e_1$.

For $e_1 > 1$, NO emissions are an increasing function of the primary airflow. NO formation occurs in the primary zone and is strongly dependant on the local concentration of oxygen into the primary zone of combustion, thus on $e_1$. The NO yields of the primary zone dominate the global NO production because NO cannot be oxidised entirely in the secondary zone, thus leading to global NO production being an overall increasing function of $e_1$.

In a similar manner, the influence of $e_2$ on the NO emissions has been studied. As in the previous case, all other parameters ($e_1$, $T_1$ and $T_2$) remained unchanged from the baseline condition, while $e_2$ was changed systematically. The results are presented in Fig. 15.

The influence of $e_2$ on the global NO production is weak for all conditions studied. In all cases global NO production appears as a decreasing function of $e_2$. The primary role of $e_2$ is to oxidize the NO produced in the primary zone. Therefore an increase in local oxygen concentration results in a decrease in the global output of NO. The effect is weak because the residence time within the reactor remains within a narrow range as the value of $e_2$ changes. Fig. 15 shows that for cases where $e_1 < 1$ (filled symbols) global NO production is an increasing function of $e_2$. As indicated before, in these conditions production and oxidation of NO occur in the secondary zone, so an increasing presence of oxygen results in an overall increase in NO. An increase of the secondary air favours the

**Table 1**
Initial conditions used for the parametric study.

| | *A* | *B* | *C* | *D* | *E* | *F* | *G* | *H* | *I* | *J* | *K* | *L* |
|---|---|---|---|---|---|---|---|---|---|---|---|---|
| Experimental primary excess air | 0.7 | 0.7 | 0.8 | 0.8 | 1 | 1 | 1 | 1.1 | 1.1 | 1.4 | 1.4 | 1.8 |
| Experimental secondary excess air | 0.6 | 0.8 | 0.6 | 0.8 | 0.7 | 0.8 | 0.9 | 0.7 | 0.9 | 0.8 | 1 | 0.8 |
| Experimental temperature in the primary zone (K) | 1123 | 1143 | 1198 | 1148 | 1248 | 1238 | 1253 | 1113 | 1233 | 1153 | 1293 | 1213 |
| Experimental temperature in the secondary zone (K) | 1223 | 1238 | 1233 | 1263 | 1273 | 1288 | 1318 | 1263 | 1283 | 1233 | 1303 | 1213 |
| Recorded fuel consumption time (s) | 420 | 440 | 430 | 415 | 470 | 470 | 465 | 400 | 485 | 500 | 500 | 540 |

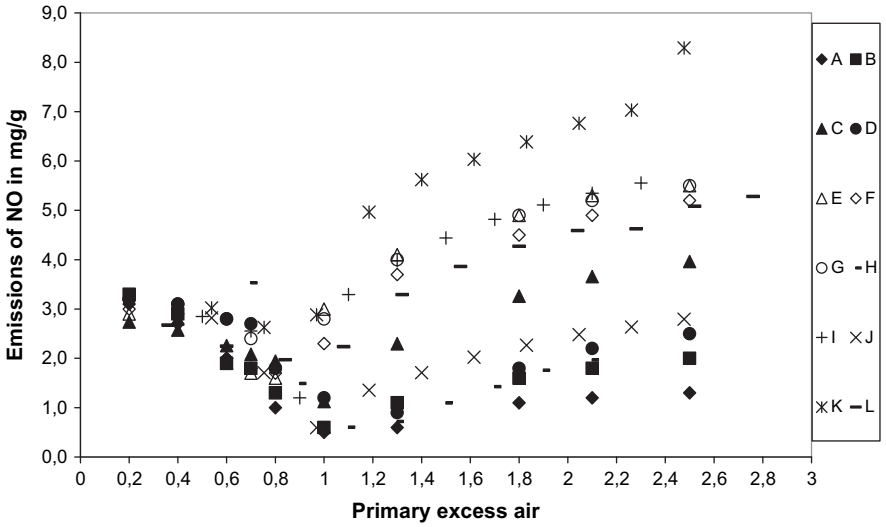


**Fig. 14.** Evolution of the NO emissions as a function of the primary excess air.

oxidation of HCN, $NH_3$ and HNCO but also of the radicals NH, HNO and NCO to form NO. In those conditions, an increase of the secondary excess air generates an increase of the NO emissions. $e_2 = 0.4$ seems to be a critical condition beyond which oxidation dominates over NO formation leading to global NO production being a weakly decreasing function of $e_2$.

The previous results indicate the dominance of the primary air in the formation of NO and the weaker effect of the secondary air in the oxidation of this specie. Nevertheless, for the previous parametric studies, the temperatures have been left at their original baseline values. The influence of the temperature in the reaction rates is well known [5,7], thus it is necessary also to explore these variables. A sensitivity analysis was therefore conducted varying independently the temperature in the primary zone within a range of $1100\,\mathrm{K} < T_1 < 1300\,\mathrm{K}$ and the secondary zone between $1150\,\mathrm{K} < T_2 < 1300\,\mathrm{K}$. The ranges were chosen to cover all observed experimental values.

As expected, Fig. 16 shows that global production of NO increases with temperature. Two clear regimes appear, that corresponding to conditions where $e_1$ is less than unity, where the change is minor and cases where $e_1 \geq 1$ where the increase in global NO production is significantly stronger. The presence of these two regimes is clear, since for $e_1 < 1$, NO formation and oxidation occurs mostly in the secondary zone of combustion, thus the increase in temperature in the primary zone affects these reactions only in as much as it increases the initial enthalpy entering the secondary zone of combustion. For conditions associated with $e_1 \geq 1$ (unfilled symbols) there is a regime where temperature has no effect on the reactions followed by a rapid increase. The critical temperature at which conditions change depends strongly on the magnitude of $e_1$. For the lower values of $e_1$ the change occurs later. This again, is an expected outcome of the sensitivity analysis, because as the temperature and rate of the reactions increase the production of NO is completed more within the primary combustion zone and the influence of its temperature is more significant. For cases where $e_1 = 1$, there is enough oxygen to proceed with the reactions but local oxygen concentrations are low and for $T_1 < 1180\,\mathrm{K}$ oxidation and reduction reactions appear to be in equilibrium, so the reaction rates are weak and NO formation occurs partially in the secondary zone.

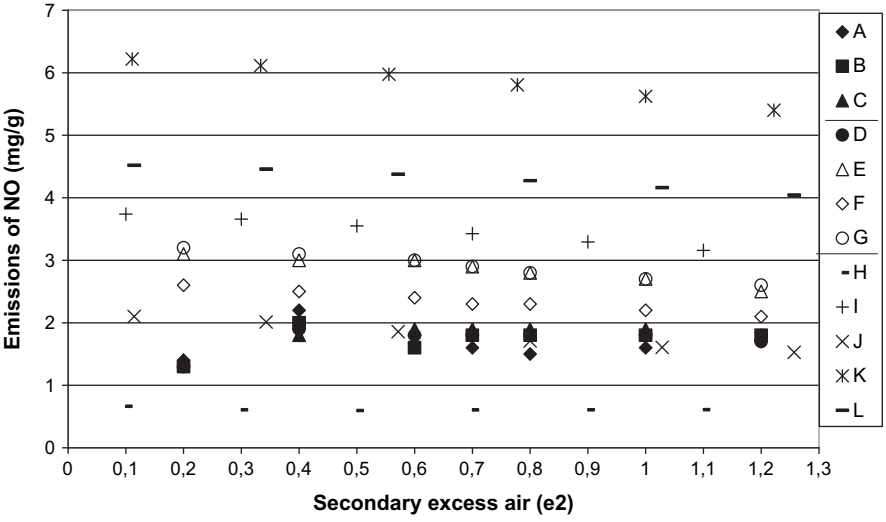


**Fig. 15.** Evolution of NO emissions as a function of the secondary excess air.

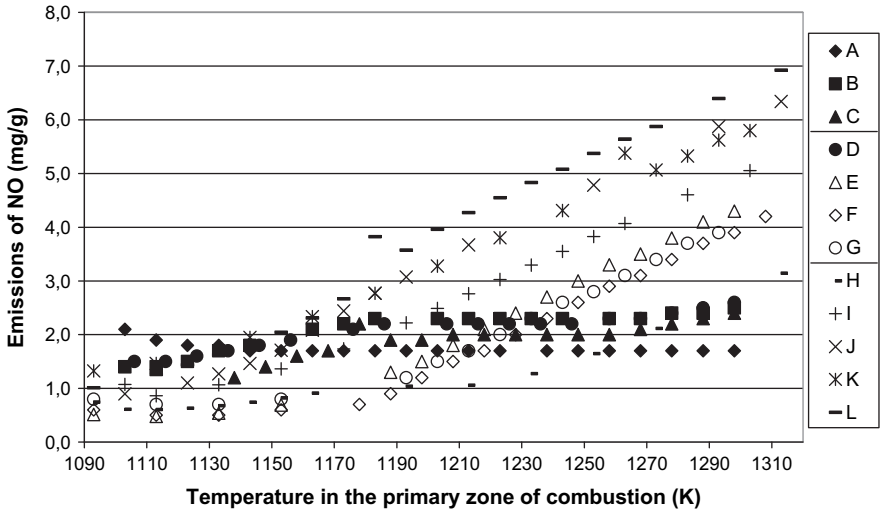


**Fig. 16.** Impact of the temperature in the primary zone of combustion on the NO emissions.

Fig. 17 shows the inverse scenario where the temperature of the secondary zone of combustion has a significant effect for the lower values of $e_1$. An interesting exception is the baseline condition (*J*) where $e_1$ is the largest. It appears that the residence time in the primary zone is too short for all reactions to be completed and some of them are carried to the secondary zone of combustion. It is interesting to note that for baseline conditions corresponding to $e_1 > 1$ the temperature of the secondary zone of combustion has almost no effect on the global NO production.

## 5. Conclusions

A computational model was developed to study the production of pollutants during the incineration of a fuel mixture that resembles urban waste. The results of the model have been compared with experiments conducted in a fixed-bed reactor that allows for primary and secondary air injection. Experimental results and model predictions showed good qualitative agreement for total oxygen consumption, NO and $CO_2$ production.

First, the numerical model has been used to establish the primary chemical pathways and their occurrence at each specific location within the reactor. The results obtained demonstrate that the NO formation and consumption depends mainly on the value of the excess air in the first zone of combustion: $e_1$. This is in agreement with previous experimental studies.

A parametric study was then conducted with the model to establish the influence of each individual variable while keeping all others constant. This parametric study is limited by the nature of the process that couples temperatures, air supply and fuel gasification rates, nevertheless, the uncoupling of these parameters gives a clear sense of the influence of each variable.

The main conclusion of the parametric study is that the initial formation of NO is controlled mainly by local oxygen concentration and only if enough oxygen is present there is an effect of the local temperature. For $e_1 \geq 1$ NO formation occurs mainly in the primary zone of combustion and the temperature of this zone has a significant effect on the global output of NO. For $e_1 < 1$, NO formation takes place mostly in the secondary zone of combustion since the local oxygen concentration in the primary zone of combustion is not sufficient to achieve the complete oxidation of the precursor species. Under these conditions the temperature of the secondary zone of combustion has a significant effect on NO production.

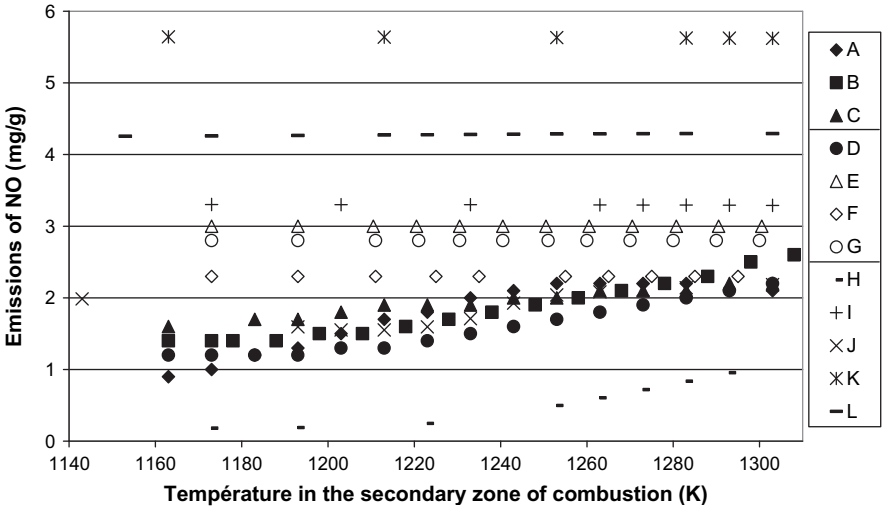


**Fig. 17.** Evolution of the NO emissions as a function of the temperature in the secondary zone of combustion.

The sensitivity study showed that NO reduction in the secondary zone of combustion has a weak dependency on temperature. Furthermore, the sensitivity study unveiled some minor effects associated to the residence time. The effect of residence time was not studied in the present work since the experimental conditions only covered this parameter in a narrow range.

## Acknowledgements

The financial support for this work was provided by the Agence De l'Environnement et de la Maitrise de l'Energie (ADEME) and by the Centre de Recherche pour l'Environnement l'Energie et le Déchet (CREED).

## References

[1] J.P. Olier, Les oxydes d'azote – Préface, Revue Générale de Thermique (1989) 330–331.
[2] T. Abbas, T, P. Costen, F.C. Lockwood, A review of current $NO_x$ control methodologies for municipal solid waste combustion process, in: Fourth European Conference on Industrial Furnaces and Boilers, London, 1997.
[3] S. Kim, D. Shin, S. Choï, Comparative evaluation of municipal solid waste incinerator designs by flow recirculation, Combustion and Flame 106 (1996) 241–251.
[4] D. Shin, S. Choï, The combustion of simulated waste particles in a fixed bed, Combustion and Flame 121 (2000) 167–180.
[5] G.G. De Soete, Mécanismes de formation et de destruction des oxydes d'azote dans la combustion, Revue Générale de Thermique (1989) 330–331.
[6] L. Sorum, O. Skreiberg, P. Glarborg, A. Jensen, K.D. Dam Johansen, Formation of NO from combustion of volatiles from municipal solid wastes, Combustion and Flame 123 (2001) 195–212.
[7] J.A. Miller, C.T. Bowman, Mechanism and modeling of nitrogen chemistry in combustion, Progress in Energy and Combustion Science 15 (1989) 287–338.
[8] T. Rogaume, M. Auzanneau, F. Jabouille, J.C. Goudeau, J.L. Torero, The effects of different airflows on the formation of the pollutants during waste incineration, Fuel 82 (2002) 2277–2288.
[9] T. Rogaume, M. Auzanneau, F. Jabouille, J.C. Goudeau, J.L. Torero, Computational model to investigate the effect of different airflows on the formation of pollutants during waste incineration, Combustion Science and Technology 175 (2003) 1501–1533.
[10] T. Rogaume, M. Auzanneau, F. Jabouille, J.C. Goudeau, J.L. Torero, Computational model to investigate the mechanisms of formation of $NO_x$ during waste incineration, Combustion Science and Technology 176 (2004) 925–943.
[11] X. Deglise, Les conversions thermochimiques du bois, Revue Forestière Française 4 (1982) 249–270.
[12] D. Fortsch, F. Kluger, U. Schnell, H. Spliethoff, K.R.G. Hein, A kinetic model for the prediction of NO emissions from combustion of pulverized coal, in: 27th International Symposium on Combustion, The Combustion Institute, 1998, pp. 3037–3044.
[13] A. Antifora, T. Faravelli, N. Kandamby, E. Ranzi, M. Sala, L. Vigevano, Comparison between two complementary approaches for predicting $NO_x$ emissions in the furnaces of utility boilers, in: Fifth International Conference on Technologies and Combustion for a Clean Environment, Lisbon, Portugal, 1999.
[14] V. Vitali, V. Lissianski, V.M. Zamansky, P.M. Maly, M.S. Sheldon, Optimisation of advanced reburning via modeling, in: 28th International Symposium on Combustion, The Combustion Institute, 2000, pp. 2475–2482.
[15] S. Goel, A. Sarofim, P. Kilpinen, M. Hupa, Emissions of nitrogen oxides from circulating fluidised bed combustors: modeling results using detailed chemistry, in: 27th International Symposium on Combustion, The Combustion Institute, 1996, pp. 3317–3324.
[16] R.J. Kee, F.M. Rupley, J.A. Miller, Chemkin-II: a Fortran Chemical Kinetics Package for the Analysis of Gas-phase Chemical Kinetics, Sandia Report, No 89–8009B, 1989.
[17] P. Glarborg, M.U. Alzueta, K. Dam-Johansen, J.A. Miller, Kinetic modeling of hydrocarbons/nitric oxide interactions in a flow reactor, Combustion and Flame 115 (1998) 1–27.
[18] G.P. Smith, D.M. Golden, M. Frenklach, N.W. Moriarty, B. Eiteneer, M. Goldenberg, C.T. Bowman, R.K. Hanson, S. Song, W.C. Gardiner Jr., V.V. Lissianski, Z. Qin, GRI-MECH, version 3–11.http://www.me.berkeley.edu/gri-mech (1999).
[19] P. Dagaut, J. Luche, M. Cathonnet, The kinetics of C1 to C4 hydrocarbons-NO interactions in relation with reburning, in: The 28th International Symposium on Combustion, The Combustion Institute, 2000, pp. 2459–2466.
[20] F. Hahnel, Conception d'un réacteur à lit fluidisé pour l'étude de l'incinération de déchets, in: Application à l'étude des mécanismes de transformation de l'azote lors de la combustion du polyamide-6,6, Thèse de doctorat de l'université de Haute-Alsace, 1999.
[21] P. Glarborg, R.J. Kee, J.F. Grcar, J.A. Miller, PSR: a Fortran Program for Modelling Well-stirred Reactors, Sandia Report, No 86–8209, 1986.